ELSEVIER

International Journal of Heat and Fluid Flow 22 (2001) 315–322

International Journal of
HEAT AND
FLUID FLOW

www.elsevier.com/locate/ijhff

Effects of freestream on turbulent combined-convection boundary layer along a vertical heated plate

Yasuo Hattori [a,*], Toshihiro Tsuji [b], Yasutaka Nagano [c], Nobukazu Tanaka [a]

[a] *Hydraulics Department, Central Research Institute of Electric Power Industry, 1646 Abiko, Abiko-shi, Chiba-ken 270-1194, Japan*
[b] *Department of Mechanical Engineering, Nagoya Institute of Technology, Gokiso-cho, Showa-ku, Nagoya 466–8555, Japan*
[c] *Department of Environmental Technology, Graduate School of Engineering, Nagoya Institute of Technology, Nagoya, Japan*

Abstract

A turbulent combined-convection boundary layer, created by imposing an aiding freestream on a turbulent natural-convection boundary layer along a vertical heated plate, was examined with normal hot- and cold-wires and a particle image velocimetry (PIV), with attention to the laminarization process of the boundary layer due to the freestream effects. As the freestream velocity increases, the wall shear stress monotonously increases, whereas the local heat transfer rate suddenly decreases. The reduction in heat transfer rates and the decays in velocity and temperature fluctuations, showing the transition from turbulent to laminar, arise at $Grx/Rex \simeq 3 \times 10^6$. With the laminarization of the boundary layer, a similar change in the turbulent quantities appears independently of Grx. For instantaneous velocity vectors obtained with PIV, large-scale fluid motions, which play a predominant role in the generation of turbulence, are frequently observed in the outer layer, while quasi-coherent structures do not exist in the near-wall region. The increasing freestream then restricts large-scale fluid motions in the outer layer, and consequently the generation of turbulence is suppressed and the boundary layer becomes laminar. © 2001 Published by Elsevier Science Inc.

Keywords: Combined-convection; Turbulent flow; Convective heat transfer; Boundary layer; Laminarization; PIV measurement

1. Introduction

It has been determined that the heat transfer rate of a turbulent thermally driven boundary layer flow declines with the introduction of a weak assisting freestream, i.e., the turbulent heat transfer rate of a combined-convection boundary layer becomes smaller than that of a natural-convection boundary layer under certain conditions (Hall and Price, 1970; Kitamura and Inagaki, 1987; Inagaki and Kitamura, 1988; Patel et al., 1998). However, the mechanism for the reduction in the heat transfer rate has not been fully comprehended, owing to a lack of credible experimental data on the near-wall turbulent quantities directly controlling the heat transfer characteristics. Thus, exploration of the mechanism of suppression in turbulent heat transfer due to a weak aiding freestream remains an important subject of study (Inagaki and Kitamura, 1988).

To clarify why the heat transfer rate in such a boundary layer decreases with an increasing freestream, we investigated the turbulent characteristics of a combined-convection boundary layer along a vertical isothermally heated plate in air with an aiding freestream, which is a typical turbulent combined-convection flow (Hattori et al., 1999, 2000a,b). The turbulent quantities in this boundary layer including the wall region were measured with normal hot- and cold-wires, and these measurements led to the conclusion that the sudden reduction in heat transfer rate resulted from the transition location to turbulence moving downstream quite rapidly. Recently, Abu-Mulaweh et al. (2000) also measured the turbulent quantities with a laser Doppler velocimeter and a cold-wire anemometer, and obtained a similar conclusion.

Since the transition of boundary layers strongly depends on the magnitude of velocity fluctuations included in the freestream (Schlichting, 1979), it is important to give due consideration to the effect of disturbances in freestream on heat transfer characteristics of the turbulent combined-convection boundary layer. Nevertheless, previous experiments have not always taken sufficient care to eliminate fluctuations in the freestream, and there is no quantitative agreement among the reported results, even as to the heat transfer rate. Combined-convection boundary layer flows are frequently encountered in engineering applications (Krishnamurthy and Gebhart, 1989; Tewari and Jaluria, 1990). The accurate estimation of reductions in the heat transfer rate is particularly indispensable in safety and rational designs for electric power constructions, such as spent fuel storage facilities, in which the decay heat of spent fuel is principally removed by combined-convection flow (Hattori et al., 1995; Sakamoto et al., 2000). Thus, correlations for evaluating the heat transfer rate in the combined-convection boundary layer have been eagerly awaited.

* Corresponding author. Tel.: +81-471-82-1181; fax: +81-471-84-7142.
E-mail address: yhattori@criepi.denken.or.jp (Y. Hattori).

0142-727X/01/$ - see front matter © 2001 Published by Elsevier Science Inc.
PII: S0142-727X(01)00094-7

Notation

$F(u), F(t)$	flatness factors of u and t
Grx	local Grashof number, $Grx = g\beta\Delta T_w x^3/\nu^2$
g	gravitational acceleration
h	heat transfer coefficient
Nux	local Nusselt number, $Nux = hx/\lambda$
Rex	local Reynolds number, $Rex = U_\infty x/\nu$
Rix	local Richardson number, $Rix = Grx/Rex^2$
R_{ut}	cross-correlation coefficient between u and t, $R_{ut} = \overline{ut}/\left(\overline{u^2}\right)^{1/2}\left(\overline{t^2}\right)^{1/2}$
$S(u)$, $S(t)$	skewness factors of u and t
T	mean temperature
t	temperature fluctuation
U	mean streamwise velocity
U_m	maximum velocity along flat plate
u	streamwise velocity fluctuation
v	transverse velocity fluctuation (perpendicular to flat plate)
x	distance from leading edge of flat plate
y	distance perpendicular to flat plate

Greeks

β	coefficient of volume expansion
λ	thermal conductivity
ν	kinematic viscosity
τ	time
τ_w	wall shear stress

Superscript and subscripts

$\overline{\ }$	time-averaged quantities
w	wall condition
∞	ambient condition

In the present study, the effects of an aiding freestream, especially a weak freestream, on the turbulent characteristics of the combined-convection boundary layer along a vertical heated plate in air were investigated. To comprehend the essential characteristics of a turbulent combined-convection boundary layer, the velocity fluctuations in the freestream were reduced to the lowest possible level, and measurements were taken using normal hot- and cold-wires and a particle image velocimetry (PIV). The change in turbulent quantities due to the laminarization of the combined-convection boundary layer was examined in detail. The experimental results clearly demonstrate the thermal and flow conditions leading to the laminarization and the stabilizing behavior of the boundary layer.

2. Experimental apparatus and procedure

The experimental apparatus consists of a vertical wind tunnel, heaters and measurement instruments (Hattori et al., 1999, 2000a). A heated plate generating a buoyancy flow (4 m high and 0.8 m wide) was installed vertically in the test section, 1×1 m^2 in area and 6.2 m high, of the vertical wind tunnel with solid boundaries. The disturbance in the freestream in the test section was reduced with four fine mesh damping screens and a honeycomb in the settling chamber of 2×2 m^2 in area and 1 m long, which was placed upstream of the contraction cone. It was confirmed that measurements for the pure forced-convection boundary layer on a flat plate gave a critical Reynolds number of $Rex \simeq 3.5 \times 10^5$. This value corresponds to flows with an extremely small intensity of turbulence in the freestream (Schlichting, 1979). Therefore, the effect of the relative ratio of fluctuation to freestream velocity (below 0.8%) was insignificant, and an ideal uniform freestream could be obtained.

Two kinds of measurements were carried out. One was a hot-wire measurement and the other was a PIV measurement. With a probe consisting of normal hot- and cold-wires, the same as in our previous report (Hattori et al., 1999, 2000a), instantaneous velocity and temperature in the boundary layer were measured. The shape and dimensions of the probe were determined to minimize measurement errors. After analog to digital conversion of output signals from the hot- and cold-wires, the instantaneous velocity and temperature were calculated with digital processing. The temperature compensation of the hot-wire and the improvement for frequency response of the cold-wire were performed in accordance with the thermal-equilibrium equations for two fine wires proposed by Hishida and Nagano (1978). Furthermore, the measurement error caused by the streamwise displacement between the wires was eliminated by delaying the temperature signals of the cold-wire according to Taylor's hypothesis (Tsuji and Nagano, 1988a). Then, the instantaneous velocity was obtained with a calibration curve that accounted for the buoyancy effects.

The PIV was measured in order to observe instantaneous two-dimensional velocity fields. Plastic microspheres of about 30 μm in diameter (Japan Fillite: EXPANCEL461DE) were added to the boundary layer flow as tracer particles. Laser light sheets were formed with a double pulse YAG laser (New Wave Research: DPIV-N90-30) and sheet-forming optical lens, and two-dimensional velocity fields in the streamwise–transverse (x–y) or streamwise–spanwise (x–z) planes were visualized. Particle-containing flow images of about 0.2×0.2 m^2 in area were captured by a CCD camera (Sony: XC-003) with a wide-angle lens (f 20/F 2.8), which was fixed at $x = 2.965$ m. The NTSC image-outputs were recorded on a laser disc (Sony: CRV-3000AN) at 30 frames per second. Through a frame grabber, the NTSC composite signals were converted to digitized images of 512×480 pixels in size and 8-bit gray level, and transferred to the host memory of a NEC 266 MHz PC. Each digital TV frame was separated into two digital TV fields. Then, velocity vectors were obtained with a pattern cross-correlation method. To improve the spatial resolution, a hierarchical recursive scheme (Hu et al., 2000) was applied: after a rough estimation for large interrogation windows of 70×70 pixels, the velocity vectors were determined from small interrogation windows with a size of 20×20 pixels. In addition, a sub-pixel algorithm was used with the assumption of a Gaussian profile for the spatial correlation.

In the present study, particular attention was given to the laminarization of the turbulent boundary layer due to the addition of a weak freestream. The accuracies of the hot-wire and PIV measurements had been demonstrated in preliminary experiments carried out for a natural-convection boundary layer along a vertical heated plate. The agreement between our hot- and cold-wire measurements and the data obtained by Tsuji and Nagano (1988a,b) was excellent for turbulent quantities even in the near-wall region, assuring that the present measurements were highly accurate.

On the other hand, the turbulent quantities measured with PIV tended to be slightly larger than those measured with the hot-wire, although there was general agreement between both profiles in the boundary layer. In particular, some discrepan-

cies existed in the near-wall region and outer region of the boundary layer, where the visualized images with tracing particles could not be captured continuously, and considerable error-vectors for instantaneous velocities were calculated. Moreover, from the frequency spectra of measured velocity fluctuations, only low frequency fluctuations below 7 Hz were judged to be reliable for PIV. Thus, the discrepancies might have been due to the peak-locking vectors (Raffel et al., 1998) and error vectors, and PIV was adequate only for the observation of large-scale fluid motions.

In the experiment, the uniform surface temperature T_w was in the range of 40–100°C and the ambient fluid temperature T_∞ was somewhat different for each experiment, in the range of 23–29°C. The vertical distance x from the leading edge of the flat plate to the measuring locations changed from 0.265 to 3.765 m. Physical properties were evaluated at the film temperature $T_f = (T_w + T_\infty)/2$ except for the coefficient of volume expansion $\beta = 1/T_\infty$. The ranges of the local Reynolds number Rex and local Grashof number Grx were 0–1.9×10^6 and 1.3×10^8–3.5×10^{11}, respectively.

3. Results and discussion

3.1. Variations in turbulent quantities due to freestream effects

Fig. 1 shows the regimes of boundary layer flows, with special attention to the laminarization region, in the coordinates of the local Reynolds number Rex and local Grashof number Grx (Hattori et al., 1999, 2000a). Even though Grx is quite large, the turbulent combined-convection flow changes to laminar with an increase in the freestream velocity: the critical Grashof number indicating the transition becomes larger with increasing Reynolds number and reaches about 100 times that in pure natural-convection at $Rex \simeq 1 \times 10^5$. As shown in this figure, the transition region indicated with hatches lies in the relation $Grx \propto Rex$ under the present experimental conditions. Therefore, the Richardson number Rix $(= Grx/Rex^2)$, which is generally used to classify the regimes of buoyancy flows, may not be effective in correlating the laminarization of the turbulent combined-convection boundary layer.

The variations in local Nusselt numbers, Nux, and wall shear stresses τ_w normalized with those for the pure turbulent natural-convection boundary layer (Tsuji and Nagano, 1988a)

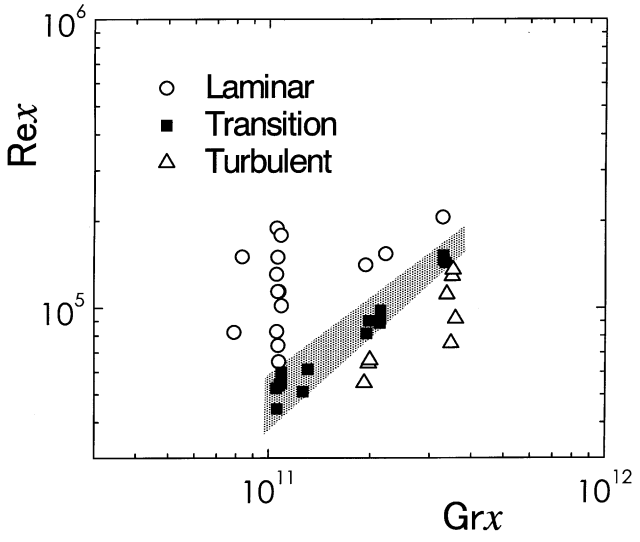

Fig. 1. Regimes of boundary layer flows.

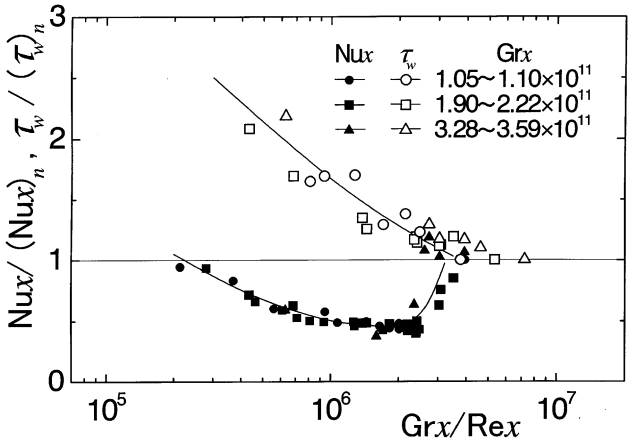

Fig. 2. Heat transfer rates and wall shear stresses with Grx/Rex.

are shown in Fig. 2 against the coordinate Grx/Rex. The heat transfer rate h and wall shear stress τ_w were estimated from velocity and temperature gradients very near the wall (Tsuji and Nagano, 1988a). It is quite evident from the figure that the parameter Grx/Rex gives good correlations for both Nux and τ_w and is suitable for evaluating the beginning point of laminarization of the boundary layer due to an increase in freestream velocity. However, the effect of the freestream on Nux differs from that on τ_w, which is attributed to a lack of analogy between heat and momentum transfer in the natural-convection boundary layer (Tsuji and Nagano, 1988a). $Nux/(Nux)_n$ suddenly decreases to about 0.4 at a given value of Grx/Rex, whereas $\tau_w/(\tau_w)_n$ increases without indicating an obvious reduction in spite of the laminarization of the boundary layer. From the results for Nux, it was presumed that the relation $Grx/Rex \simeq 3 \times 10^6$ $(Grx > 10^{11})$ may be a good guideline for predicting the occurrence of a laminarization of the turbulent combined-convection boundary layer.

Our previous study (Hattori et al., 1999, 2000a) revealed that the turbulent characteristics of the combined-convection boundary layer are different in several respects from those in both natural and forced convection. Here, concentrating on the data at $Grx/Rex \simeq 3 \times 10^6$, we examined the turbulent statistics of the combined-convection boundary layer for different Grashof numbers ($Grx = 1.95$–1.98×10^{11} and 3.28–3.59×10^{11}).

The intensity profiles of streamwise velocity fluctuation u with increasing freestream velocity are shown in Fig. 3. The intensity of velocity fluctuation u is normalized by the maximum mean velocity U_m, and a similarity variable $\eta = (y/x)Grx^{1/4}$ for the laminar natural-convection boundary layer is used as the dimensionless distance from the wall, which is suitable for scaling the flow field near the wall in the turbulent natural-convection boundary layer (Tsuji and Nagano, 1989). In pure natural-convection ($Grx/Rex = \infty$), the maximum intensity of velocity fluctuation occurs beyond the maximum mean velocity location ($\eta \simeq 3$). With the introduction of freestream ($Grx/Rex = 3.92 \times 10^6$ for $Grx \simeq 3.5 \times 10^{11}$), the boundary layer thickness becomes thinner and the maximum velocity location approaches the wall (Hattori et al., 1999, 2000a), and simultaneously the intensity of the velocity fluctuation begins to decrease. As freestream velocity increases, a similar change in the intensity profiles for different Grx is observed. At $Grx/Rex = 2.73 \times 10^6$ for $Grx \simeq 3.5 \times 10^{11}$ and $Grx/Rex = 3.08 \times 10^6$ for $Grx \simeq 2 \times 10^{11}$, the maximum values of fluctuation intensities are attained at the maximum mean velocity location ($\eta \simeq 1.5$), and these values become larger than those for pure natural-convection. Then, at

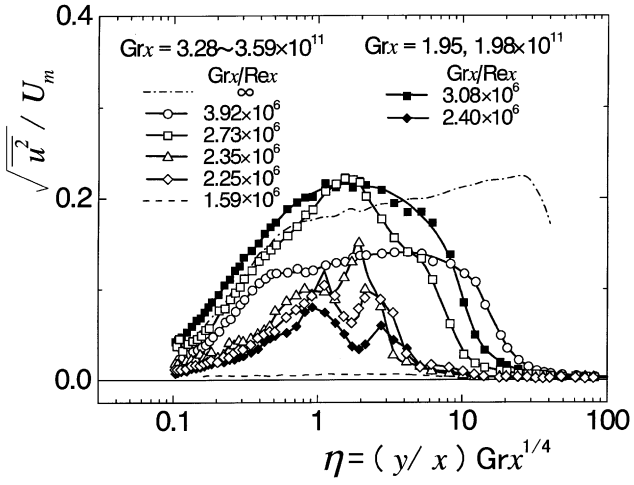

Fig. 3. Intensities of streamwise velocity fluctuation.

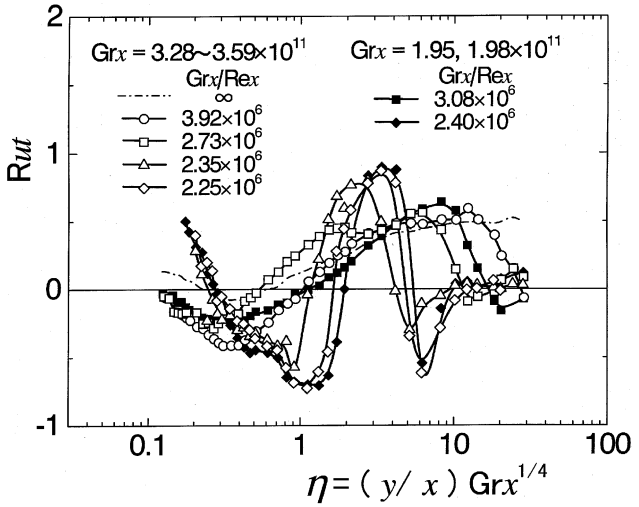

Fig. 5. Cross-correlation coefficients between velocity and temperature fluctuations.

$Grx/Rex = 2.35 \times 10^6$, 2.25×10^6 for $Grx \simeq 3.5 \times 10^{11}$ and $Grx/Rex = 2.40 \times 10^6$ for $Grx \simeq 2 \times 10^{11}$, the intensity profiles of fluctuations show two peaks with an infinitesimal value near the maximum mean velocity location, with a rapid decay in the fluctuation over the entire boundary layer region. This profile characterizes a laminarization of the turbulent combined-convection boundary layer (Carey and Gebhart, 1983; Krishnamurthy and Gebhart, 1989). A further increase in freestream velocity results in the disappearance of velocity fluctuation with the laminarization of the boundary layer.

Fig. 4 presents the change in the intensity of the temperature fluctuation t normalized by the temperature difference between the surface temperature T_w and the ambient temperature T_∞ with increasing freestream velocity. Regardless of Grx values, the increasing and decreasing tendencies of the maximum intensity of the temperature fluctuation closely resemble those of velocity fluctuation: the maximum intensity of the temperature fluctuation decreases with the introduction of a freestream, and as the freestream velocity increases, the maximum value initially increases and then rapidly decreases with the transition from turbulent to laminar.

The change in the cross-correlation coefficients R_{ut} between velocity and temperature fluctuations is presented in Fig. 5. The profile of R_{ut} also varies remarkably due to the laminarization of the boundary layer, and the peculiar profile is observed at $Grx/Rex \simeq 3 \times 10^6$. Independently of Grx, the different sign of R_{ut} alternately appears with y and the maximum absolute value of R_{ut} becomes almost unity. Since the waveforms of velocity fluctuation u and temperature fluctuation t vary from random to harmonic with a specific frequency in the laminarization of the boundary layer (Hattori et al., 2000a), this profile of R_{ut} implies that velocity and temperature fluctuations have the same frequency with different phases. The estimated phase difference between velocity and temperature fluctuations approximately coincides with that determined by a linear stability analysis for the transition of the laminar combined-convection boundary layer (Carey and Gebhart, 1983).

Consequently, it is found that the criterion for the beginning of the reduction in heat transfer rate due to the laminarization of the boundary layer may be determined by the relation $Grx/Rex \simeq 3 \times 10^6$ for $Grx > 10^{11}$. Hall and Price (1970) conducted an experiment and concluded that the heat transfer rate became minimum when the freestream velocity was of the same order of magnitude as the maximum mean velocity in the turbulent natural-convection boundary layer. Kitamura and Inagaki (1987) also made a similar report for the condition of the minimum heat transfer rate. In the present experiment, a rapid reduction in the heat transfer rate was observed at a rather small freestream velocity of about half or two thirds the maximum mean velocity. The discrepancy between the present results and those of these earlier studies may be ascribed to the differences in the experimental setup and conditions. In their experiments, test sections with small areas were used and relatively large disturbances were involved in the freestream, which yielded a substantially small transition Reynolds number value even for pure forced-convection. In fact, they did not observe an obvious laminarization of the boundary layer, though velocity fluctuations were suppressed to some extent. Thus, the occurrence of Nux reduction was not so abrupt as that observed in the present experiment and the minimum value of $Nux/(Nux)_n$ remained at about 0.75. It is considered that the present results, obtained by controlling freestream disturbances to the lowest level possible, more accurately reveal the essential characteristics of the turbulent combined-convection boundary layer.

On the other hand, Patel et al. (1998) numerically investigated the heat transfer characteristics of the combined-convection boundary layer with a low Reynolds-number k–ε

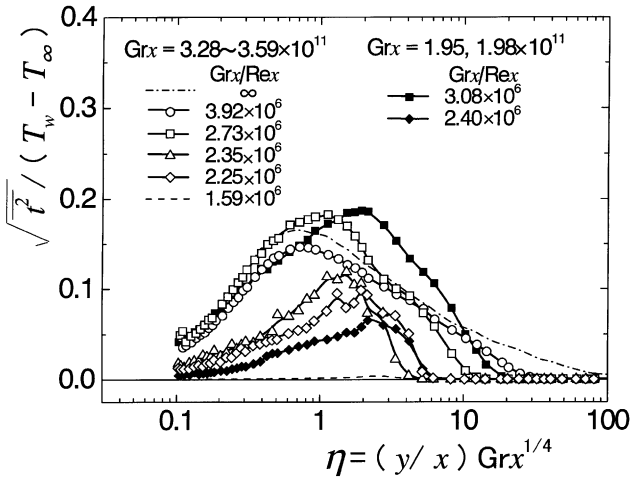

Fig. 4. Intensities of temperature fluctuation.

turbulence model. They classified various flow regimes and suggested that, with a deterioration of *Nux*, turbulent natural-convection changed to turbulent combined-convection under the condition of $Rex = 0.00174Grx^{0.615}$ ($Grx > 5 \times 10^9$). However, this criterion gives a reduction in *Nux* at a quite small *Rex* and a laminarization of the boundary layer could not be

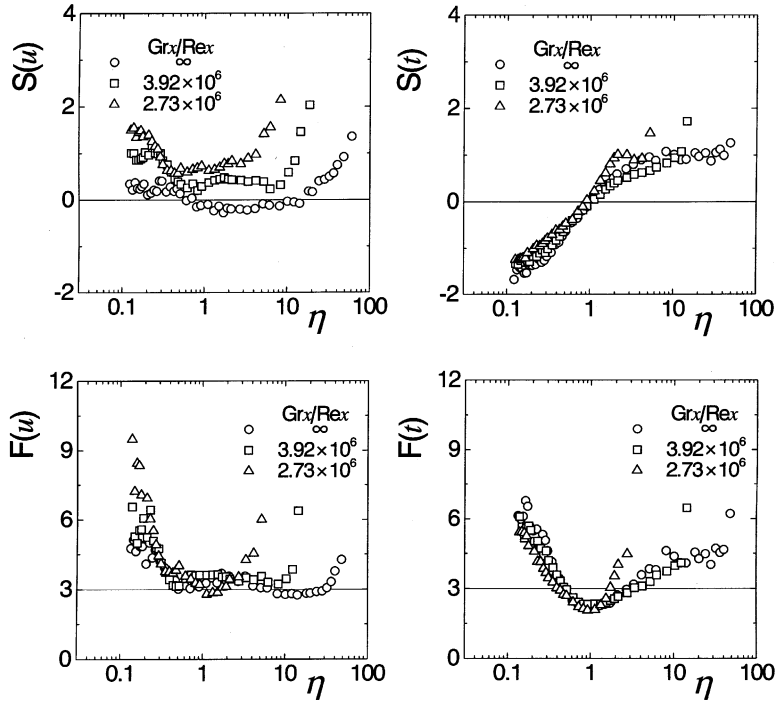

Fig. 6. Skewness and flatness factors of velocity and temperature fluctuations.

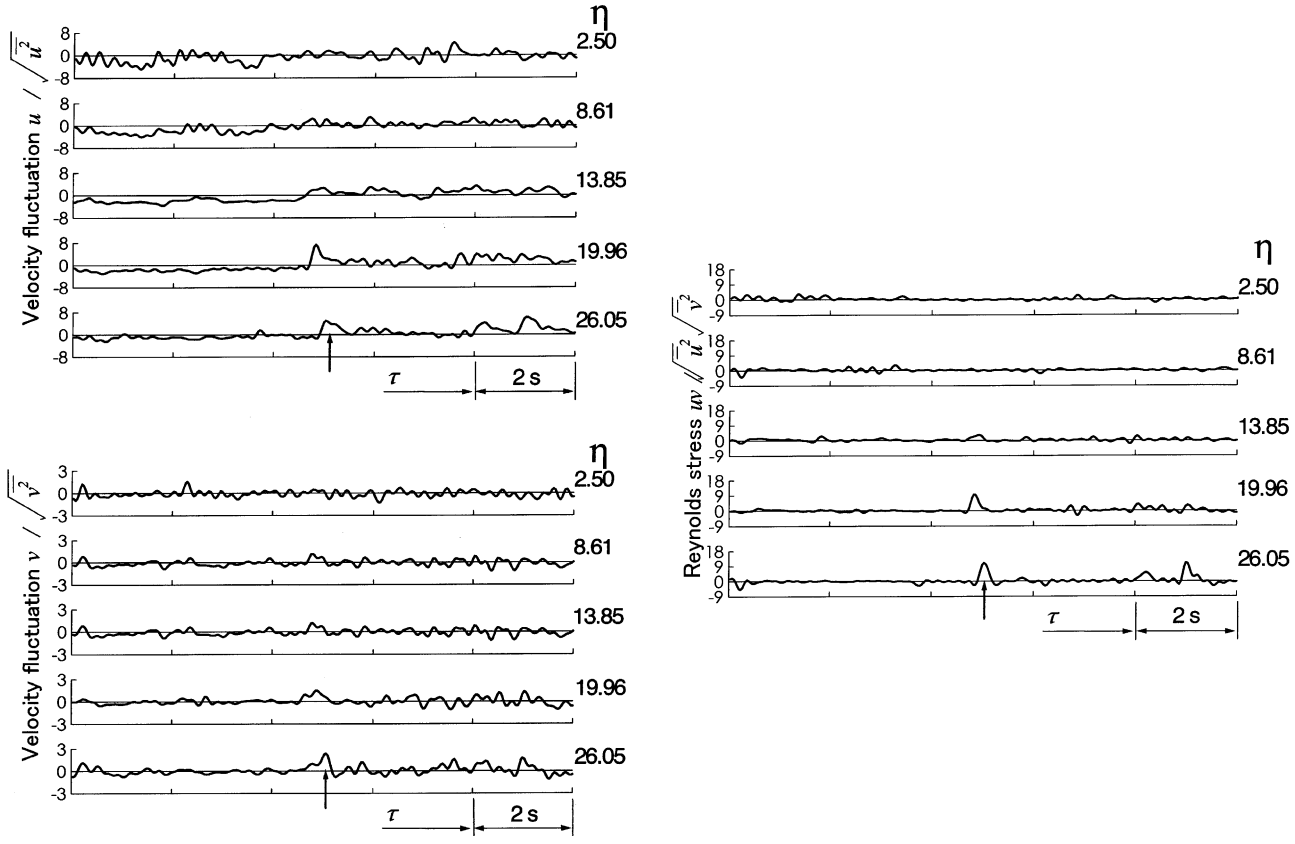

Fig. 7. Signal traces of velocity fluctuations *u* and *v* and Reynolds stresses *uv*.

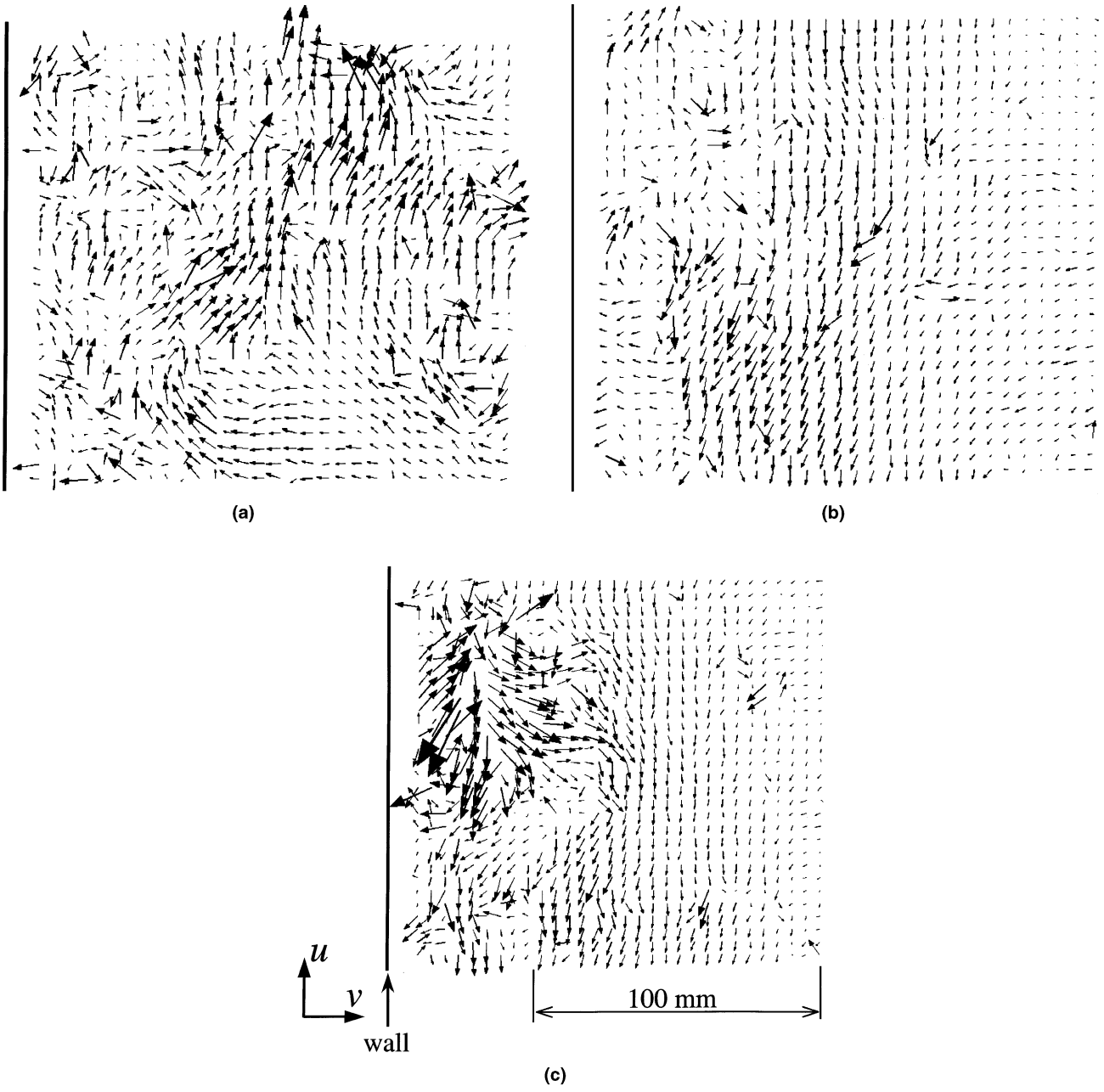

Fig. 8. Velocity fluctuation vectors in $(x$–$y)$ plane: (a) $uv > 0$; (b) $uv \simeq 0$; (c) $uv < 0$.

predicted, which may disclose a deficiency in existing turbulence models.

3.2. Turbulent behavior

The behavior of higher order correlations in the boundary layer was examined to understand more clearly the stabilizing effect of the freestream on the combined-convection boundary layer. The skewness factors $S(u)$ and $S(t)$ and the flatness factors $F(u)$ and $F(t)$, which are third- and fourth-order moments of velocity and temperature fluctuations, respectively, are presented in Fig. 6. These factors are definitely different from those for the Gaussian probability distribution, and the factors for pure natural-convection agree closely with measurements by Tsuji and Nagano (1988b). The effect of freestream sensitively appears in the velocity field. As freestream velocity increases, the mean velocity profile in the boundary layer markedly varies (Hattori et al., 1999, 2000a). Simultaneously, $S(u)$ shift towards positive while the velocity fluctuation has a probability distribution close to Gaussian ($S(u) \simeq 0$ and $F(u) \simeq 3$) over a wide range of the natural-convection boundary layer. Near the wall, $F(u)$ becomes substantially higher than in pure natural-convection, which indicates more intermittent fluctuations. On the other hand, the changes in $S(t)$ and $F(t)$ profiles are relatively small. All the skewness factors $S(t)$ of temperature fluctuation become negative near the wall ($\eta < 1$) and positive in the outer layer ($\eta > 1$), and all the flatness factors $F(t)$ near the wall and the outer edge of the boundary layer exceed a value of 3. These profiles of skewness and flatness factors characterize high- and low-temperature fluid motions encompassing the whole boundary layer region as observed in the natural-convection

boundary layer (Tsuji et al., 1992; Tsuji and Nagano, 1996). Thus, the large-scale structure in the outer layer, which is strongly connected with a turbulence generation in the natural-convection boundary layer, seems to be also maintained in the combined-convection boundary layer despite the addition of a freestream.

Fluid motions in the outer layer of the combined-convection boundary layer at $Grx/Rex = 3.44 \times 10^6$ for $Grx = 1.1 \times 10^{11}$ were investigated with PIV measurements. Fig. 7 shows instantaneous signals of velocity fluctuations u and v together with the Reynolds shear stresses uv normalized by the relevant fluctuation intensities. The form of the signals changes with the distance from the wall η. As the outer edge of the boundary layer is approached, long-period signals become notable, while high-frequency signals appear at the maximum mean velocity location. Intermittent occurrences of strong positive u motion, which concern the profiles of skewness and flatness factors shown in Fig. 6, simultaneously induce v and uv motions of large positive values. Such fluid motions generate turbulent energy, since the mean velocity gradient in the outer layer is negative.

Fig. 8 shows instantaneous fluctuation velocity fields in the $(x–y)$ plane captured at $uv > 0$, $uv \simeq 0$ and $uv < 0$ marked with arrows in Fig. 7. The features of the motion of each fluid are strikingly different. When uv takes a positive value, it is frequently observed that a large-scale fluid motion with a high-speed moves from the maximum mean velocity location toward the edge of the boundary layer. Compared with such a fluid motion, the scale of the fluid motion at $uv < 0$ is quite small and the occurrence of large amplitude fluctuations is limited to the region around the maximum mean velocity location. This result demonstrates that the scale of the outward fluid motion with a high-speed contributing to the generation of turbulence is distinctly larger than that of other fluid motions.

Fig. 9 demonstrates the temporal variation in instantaneous streamwise velocity profile in the boundary layer when turbulent energy is generated. Over the entire boundary layer, the velocity profile is initially lower than the time-averaged velocity and then increases with time. Such a change in the velocity field from a low-speed flow to a high-speed flow can be regarded as fluid motions responding to the large-scale structure in the thermal field, because the cross-correlation coefficient between streamwise velocity and temperature fluctuations takes a high value of about 0.6 in the outer layer of the combined-convection boundary layer, as shown in Fig. 5.

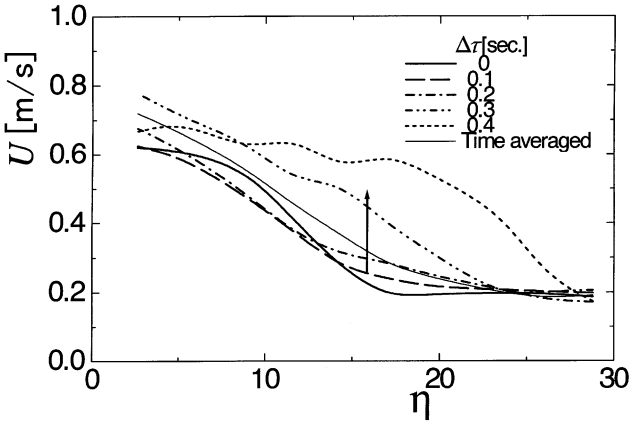

Fig. 9. Temporal variation of instantaneous streamwise velocity profile in $(x–y)$ plane.

For the turbulent combined-convection boundary layer, the time series of instantaneous vectors consisting of velocity fluctuations u and w observed near the wall ($\eta \simeq 0.8$, $y \simeq 4$ mm) are shown in Fig. 10. In the ordinary boundary layer, turbulence generation is associated with the quasi-coherent structure near the wall, such as low- and high-speed streaks (Kim et al., 1987). However, no streaky structure could be recognized in the visualized fluid motions with PIV for the turbulent combined-convection boundary layer. Tsuji et al. (1992), and Tsuji and Nagano (1996) concluded through measurements with a thermocouple rake and flow visualization using a smoke-wire technique that low- and high-speed streaks and intermittent bursts as seen in forced-convection did not exist near the wall in the turbulent natural-convection boundary layer. Velocity vectors obtained for the combined-convection boundary layer also suggest a lack of quasi-coherent structures. Because a laminarization of the boundary

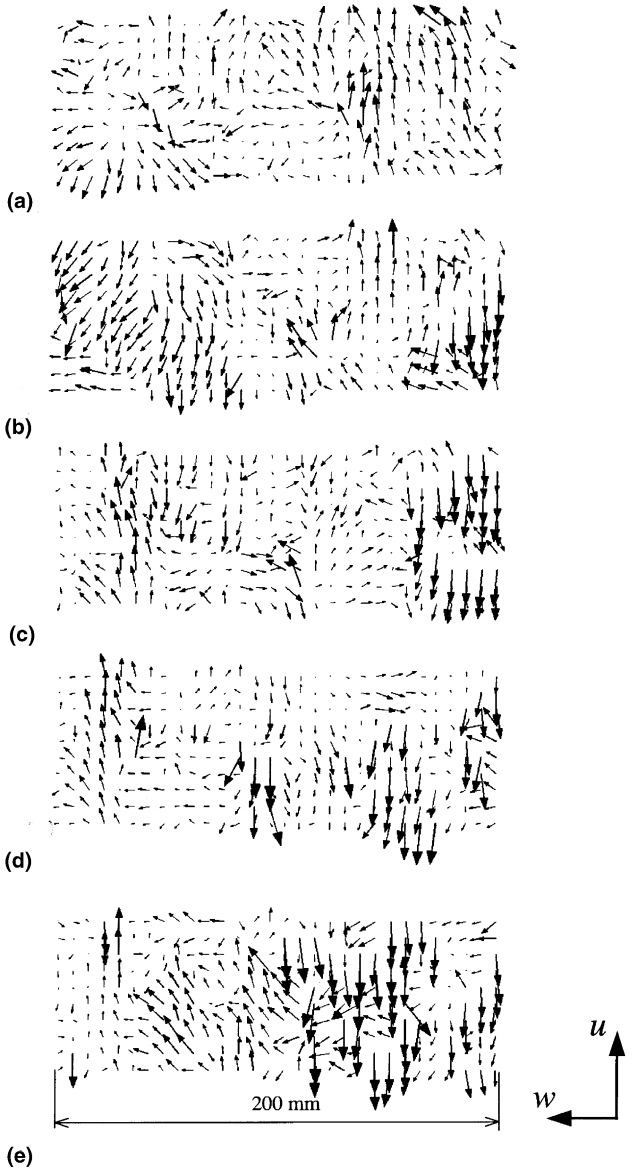

Fig. 10. Velocity fluctuation vectors in $(x–z)$ plane in near-wall region: (a) $\Delta\tau = 0/30$ (s); (b) $\Delta\tau = 1/30$ (s); (c) $\Delta\tau = 2/30$ (s); (d) $\Delta\tau = 3/30$ (s); (e) $\Delta\tau = 4/30$ (s).

layer occurs with a slight increase in freestream, it may be conjectured that the combined-convection boundary layer in itself does not have any quasi-coherent structure.

From these results, in the combined-convection boundary layer, it is found that the large-scale structure in the outer region plays a predominant role in turbulence generation, whereas no quasi-coherent structure exists in the near-wall region. Therefore, a slight increase in uniform freestream added at the outer edge of the boundary layer may restrict the large-scale vortex motions that serve to maintain turbulence in the outer layer, and bring on a laminarization of the boundary layer.

4. Conclusions

Measurements with normal hot- and cold-wires and a PIV were conducted to investigate the laminarization of the turbulent combined-convection boundary layer, which is created by imposing an aiding freestream on a turbulent natural-convection boundary along a vertical heated plate.

The results obtained may be summarized as follows:

1. As the freestream velocity increases, the wall shear stress monotonously increases, whereas the local heat transfer rate suddenly decreases due to a laminarization of the boundary layer.
2. Flow and heat transfer characteristics with the laminarization of the turbulent combined-boundary layer are correlated with the unique parameter Grx/Rex, and the laminarization occurs at $Grx/Rex \simeq 3 \times 10^6$ for $Grx > 10^{11}$.
3. For the turbulent combined-convection boundary layers, the large-scale fluid motions in the outer region play a predominant role in turbulence generation, while quasi-coherent structures as observed in the ordinary boundary layers do not exist in the near-wall.
4. An increasing freestream restricts large-scale fluid motions in the outer layer, so that turbulence generation is suppressed and the boundary layer becomes laminar.

References

Abu-Mulaweh, H.I., Chen, T.S., Armaly, B.F., 2000. Effects of stream velocity on turbulent natural convection flow along a vertical plate. Exp. Heat Transfer J. 13, 183–195.

Carey, V.P., Gebhart, B., 1983. The stability and disturbance amplification characteristics of vertical mixed convection flow. J. Fluid Mech. 127, 185–201.

Hall, W.B., Price, P.H., 1970. Mixed forced and free convection from a vertical heated plate to air. In: Proceedings of the Fourth International Heat Transfer Conference, vol. 4, NC 3.3.

Hattori, Y., Kashiwagi, E., Yamakawa, H., Wataru M., 1995. Experiments of natural convection to evaluate heat transfer in the spent fuel dry storage facilities. In: Proceedings of the Third International Conference on Nuclear Engineering, vol. 4, pp. 1927–1932.

Hattori, Y., Tsuji, T., Nagano, Y., Tanaka, N., 1999. Characteristics of turbulent combined-convection boundary layer along a vertical heated plate. In: Proceedings of the First Symposium on Turbulence and Shear Flow Phenomena, pp. 545–550.

Hattori, Y., Tsuji, T., Nagano, Y., Tanaka, N., 2000a. Characteristics of turbulent combined-convection boundary layer along a vertical heated plate. Int. J. Heat Fluid Flow 21, 520–525.

Hattori, Y., Tsuji, T., Nagano, Y., Tanaka, N., 2000b. Retransition from turbulence to laminar flow in a combined-convection boundary layer along a vertical heated plate. In: Proceedings of the Fourth JSME-KSME Thermal Engineering Conference, pp. 3-187–3-192.

Hishida, M., Nagano, Y., 1978. Simultaneous measurements of velocity and temperature in nonisothermal flows. ASME J. Heat Transfer 100, 340–345.

Hu, H., Saga, T., Kobayashi, T., Taniguchi, N., Segawa, S., 2000. Visualization on the small scale vortices in a jet mixing flow by using hierarchical recursive PIV method. In: Proceedings of the Sixth JSME Kanto branch General Meeting, pp. 173–174 (in Japanese).

Inagaki, T., Kitamura, K., 1988. Turbulent heat transfer of combined forced and natural convection along a vertical flat plate (Effect of Prandtl number). JSME B 54, 2515–2522 in Japanese.

Kim, J., Moin, P., Moser, R., 1987. Turbulence statistics in fully developed channel flow at low Reynolds number. J. Fluid Mech. 177, 133–166.

Kitamura, K., Inagaki, T., 1987. Turbulent heat and momentum transfer of combined forced and natural convection along a vertical flat plate – Aiding flow. Int. J. Heat Mass Transfer 30, 23–41.

Krishnamurthy, R., Gebhart, B., 1989. An experimental study of transition to turbulence in vertical mixed convection flows. ASME J. Heat Transfer 111, 121–130.

Patel, K., Armaly, B.F., Chen, T.S., 1998. Transition from turbulent natural to turbulent forced convection. ASME J. Heat Transfer 120, 1086–1088.

Raffel, M., Willert, C., Kompenhans, J., 1998. Particle Image Velocimetry. Springer, Berlin.

Sakamoto, K., Koga, T., Wataru, M., Hattori, Y., 2000. Heat removal characteristics of vault storage system with cross flow for spent fuel. Nucl. Eng. Des. 195, 57–68.

Schlichting, H. (Ed.), 1979. Boundary-Layer Theory. Mcgraw-Hill, New York, pp. 572.

Tewari, S.S., Jaluria, Y., 1990. Mixed convection heat transfer from thermal sources mounted on horizontal and vertical surfaces. ASME J. Heat Transfer 112, 975–987.

Tsuji, T., Nagano, Y., 1988a. Characteristics of a turbulent natural convection boundary layer along a vertical flat plate. Int. J. Heat Mass Transfer 31, 1723–1734.

Tsuji, T., Nagano, Y., 1988b. Turbulence measurements in a natural convection boundary layer along a vertical flat plate. Int. J. Heat Mass Transfer 31, 2101–2111.

Tsuji, T., Nagano, Y., 1989. Velocity and temperature measurements in a natural convection boundary layer along a vertical flat plate. Exp. Thermal Fluid Sci. 2, 208–215.

Tsuji, T., Nagano, Y., Tagawa, M., 1992. Experiment on spatio-temporal turbulent structures of a natural convection boundary layer. ASME J. Heat Transfer 114, 901–908.

Tsuji, T., Nagano, Y., 1996. Structural characteristics of a turbulent natural convection boundary layer. In: Proceedings of the Second China–Japan Work Shop Turbulent Flows, pp. 277–289.